

**LNF-96/055**

## **Coupling Impedance of a Hole in a Coaxial Beam Pipe**

S. De Santis, M. Migliorati, L. Palumbo, M. Zobov

*Physical review E, 54, N. 1, 800-805, (1996)*

## Coupling impedance of a hole in a coaxial beam pipe

S. De Santis,<sup>1,2</sup> M. Migliorati,<sup>2</sup> L. Palumbo,<sup>1,2,\*</sup> and M. Zobov<sup>2</sup>

<sup>1</sup>Dipartimento di Energetica—University of Rome “La Sapienza,” Rome, Italy

<sup>2</sup>INFN—Laboratori Nazionali di Frascati, Cassella Postale 13 00044 Frascati, Italy

(Received 18 January 1996)

In this paper we derive the impedance of a circular hole in the inner tube of a coaxial beam pipe. The method used differs from the classic Bethe's diffraction theory, since, in the calculation of the magnetic and electric dipole moments, we take into account also the scattered fields in the aperture to match the power conservation law. The low-frequency impedance shows a real contribution accounting for the TEM waves propagating within the coaxial waveguide. [S1063-651X(96)09406-8]

PACS number(s): 41.75.-i, 41.20.-q

### I. INTRODUCTION

The impedance of a hole in a beam pipe has been recently thoroughly studied. Many different shapes and hole distributions have been analyzed [1–4]. The importance of such a geometry in the vacuum chamber arose in particular in the design of the Superconducting Supercollider (SSC) [5] and the Large Hadron Collider (LHC) [6,7]. At low frequencies, i.e., for wavelengths much larger than the hole size, the fields can be calculated by applying Bethe's theory, which states that the hole is equivalent to a combination of radiating electric and magnetic dipoles and their moments are related to the amplitude of the primary incident fields [8]. At first order the method yields a purely imaginary impedance [1,2]. Recently, the real part of the impedance has been calculated considering the energy radiated by the hole into the beam pipe and in the free space [9,10]. The impedance of a hole in a coaxial pipe has been calculated by Gluckstern applying Bethe's theory [3].

In this paper we improve the impedance calculations in several respects. In order to make the power conservation hold, the electric and magnetic dipole moments are calculated taking into account also the fields scattered in the circular and coaxial waveguides. Furthermore, the impedances are calculated also for a charge traveling with velocity  $\beta c$ .

At low frequency, below the cutoff of the circular and coaxial waveguides, the longitudinal impedance shows a real contribution, scaling like  $\omega^2$ , which corresponds to the TEM mode propagating inside the coaxial waveguide.

### II. GENERAL APPROACH

In this section we briefly describe the method generally used in the microwave techniques to study the coupling of two waveguides through a small aperture. In our case, however, the primary field is produced by a charge traveling off-axis with velocity  $\beta c$ . The fields are scattered by the small aperture in both the circular ( $g_i$ ) and coaxial waveguide ( $g_e$ ) (Fig. 1).

Due to the symmetry, the primary fields produced by the charge inside the circular pipe have only the components:

$E_{0r}$ ,  $E_{0z}$ , and  $H_{0\phi}$  (see Appendix A).

The scattered fields in the pipes can be represented as an infinite series of normal modes. Modes TE and TM can propagate in both the  $g_i$  and  $g_e$  waveguides, while a TEM mode (which propagates without cutoff) must be also considered in  $g_e$ .

The scattered field can be expressed as a sum of independent modes (see Appendix B). Each mode will propagate in both  $z$  directions, after scattering occurs at the aperture. Therefore we have, for waveguide  $g_i$ :

$$\mathbf{E}_i = \sum_{n,m} [a_{n,m} \mathbf{e}_{i(n,m)}^+ e^{-jk_{z(n,m)}z} \theta(z) + b_{n,m} \mathbf{e}_{i(n,m)}^- e^{jk_{z(n,m)}z} \theta(-z)], \quad (1)$$

$$\mathbf{H}_i = \sum_{n,m} [a_{n,m} \mathbf{h}_{i(n,m)}^+ e^{-jk_{z(n,m)}z} \theta(z) + b_{n,m} \mathbf{h}_{i(n,m)}^- e^{jk_{z(n,m)}z} \theta(-z)],$$

and for waveguide  $g_e$ :

$$\mathbf{E}_e = \sum_{n,m} [c_{n,m} \mathbf{e}_{e(n,m)}^+ e^{-jk_{z(n,m)}z} \theta(z) + d_{n,m} \mathbf{e}_{e(n,m)}^- e^{jk_{z(n,m)}z} \theta(-z)], \quad (2)$$

$$\mathbf{H}_e = \sum_{n,m} [c_{n,m} \mathbf{h}_{e(n,m)}^+ e^{-jk_{z(n,m)}z} \theta(z) + d_{n,m} \mathbf{h}_{e(n,m)}^- e^{jk_{z(n,m)}z} \theta(-z)],$$

where  $\theta(z)$  is the step function, and

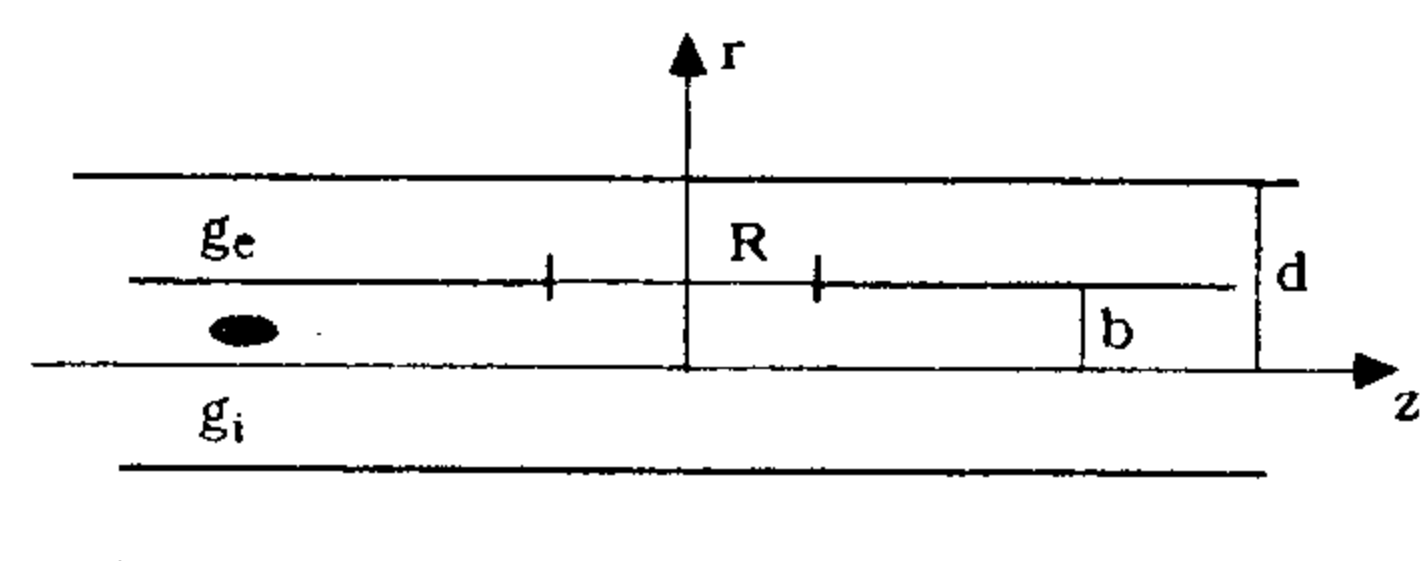


FIG. 1. Structure geometry.

\*Corresponding author.

$$\begin{aligned} \mathbf{e}_{(n,m)}^{\pm} &= \mathbf{e}_{r(n,m)} + \mathbf{e}_{\varphi(n,m)} \pm \mathbf{e}_{z(n,m)}, \\ \mathbf{h}_{(n,m)}^{\pm} &= \pm (\mathbf{h}_{r(n,m)} + \mathbf{h}_{\varphi(n,m)}) + \mathbf{h}_{z(n,m)}. \end{aligned} \quad (3)$$

The expressions of the modal functions in (3) are given in Appendix B.

To determine the coefficients  $a_{n,m}$ ,  $b_{n,m}$ ,  $c_{n,m}$ ,  $d_{n,m}$ , we make use of the Lorentz reciprocity principle, which relates the fields to the sources  $\mathbf{J}$  and  $\mathbf{J}_m$ :

$$\oint_S (\mathbf{E}_{(n,m)}^{\pm} \times \mathbf{H} - \mathbf{E} \times \mathbf{H}_{(n,m)}^{\pm}) \cdot \hat{\mathbf{n}} dS = \int \int \int \mathbf{J} \cdot \mathbf{E}_{(n,m)}^{\pm} dV,$$

$$\mathbf{E}_{(n,m)}^{\pm} = \mathbf{e}_{(n,m)}^{\pm} e^{\mp jk_z(n,m)z}, \quad (4)$$

$$\mathbf{H}_{(n,m)}^{\pm} = \mathbf{h}_{(n,m)}^{\pm} e^{\mp jk_z(n,m)z}.$$

Because of the orthogonality of the field functions (3), we get:

$$a_{n,m} = \frac{1}{2} \int \int_A \mathbf{H}_{i(n,m)}^{-} \cdot \mathbf{J}_m dS,$$

$$b_{n,m} = \frac{1}{2} \int \int_A \mathbf{H}_{i(n,m)}^{+} \cdot \mathbf{J}_m dS,$$

$$c_{n,m} = -\frac{1}{2} \int \int_A \mathbf{H}_{e(n,m)}^{-} \cdot \mathbf{J}_m dS,$$

$$d_{n,m} = -\frac{1}{2} \int \int_A \mathbf{H}_{e(n,m)}^{+} \cdot \mathbf{J}_m dS. \quad (5)$$

The coefficients of the scattered fields, in the case of a small aperture, are related to an electric and a magnetic dipole on its center.

$$a_{n,m} = \frac{j\omega}{2} (\mu \mathbf{H}_{i(n,m)}^{-} \cdot \mathbf{M} - \mathbf{E}_{i(n,m)}^{-} \cdot \mathbf{P}),$$

$$b_{n,m} = \frac{j\omega}{2} (\mu \mathbf{H}_{i(n,m)}^{+} \cdot \mathbf{M} - \mathbf{E}_{i(n,m)}^{+} \cdot \mathbf{P}),$$

$$c_{n,m} = -\frac{j\omega}{2} (\mu \mathbf{H}_{e(n,m)}^{-} \cdot \mathbf{M} - \mathbf{E}_{e(n,m)}^{-} \cdot \mathbf{P}),$$

$$d_{n,m} = -\frac{j\omega}{2} (\mu \mathbf{H}_{e(n,m)}^{+} \cdot \mathbf{M} - \mathbf{E}_{e(n,m)}^{+} \cdot \mathbf{P}). \quad (6)$$

On the other hand, these electric and magnetic dipoles are proportional to the true tangent magnetic field and normal electric field at the aperture, through the electric and magnetic polarizability coefficients  $\alpha_m$  and  $\alpha_e$ . In the static approximation, these dipole coefficients have been calculated for various aperture shapes [8,11].

The electric and magnetic dipoles are given by:

$$\begin{aligned} \mathbf{M} &= \vec{\alpha}_m \cdot (\mathbf{H}_0 + \mathbf{H}_i - \mathbf{H}_e) \Big|_{\varphi=z=0}^{r=b}, \\ \mathbf{P} &= \varepsilon \vec{\alpha}_e \cdot (\mathbf{E}_0 + \mathbf{E}_i - \mathbf{E}_e) \Big|_{\varphi=z=0}^{r=b}, \end{aligned} \quad (7)$$

where  $\mathbf{H}_i$  and  $\mathbf{H}_e$  ( $\mathbf{E}_i$  and  $\mathbf{E}_e$ ) are the tangent magnetic (electric) fields scattered in the circular and coaxial waveguide, respectively, and  $\vec{\alpha}_m$ ,  $\vec{\alpha}_e$  are the polarizability tensors.

The static solutions of  $\mathbf{P}$  and  $\mathbf{M}$ , being in phase with the fields, do not lead to power extraction from the incident wave, so that the power conservation law is violated. The modified Bethe's theory allows to find the correct expression for the dipole moments, such to balance the scattered power. In waveguide coupling problems, the leading correction term comes from the propagating modes that are excited [8].

Substituting the expressions of the fields in (7) we derive the following linear system for the dipole components:

$$\begin{pmatrix} 1 + \alpha_m \mu S_{\varphi\varphi} & \mp \alpha_m \mu S_{\varphi z} & \pm \alpha_m S_{\varphi r} \\ \pm \alpha_m \mu S_{\varphi z} & 1 - \alpha_m \mu S_{zz} & \alpha_m S_{zr} \\ \pm \frac{\alpha_e}{c^2} S_{\varphi r} & -\frac{\alpha_e}{c^2} S_{zr} & 1 + \alpha_e \varepsilon S_{rr} \end{pmatrix} \begin{pmatrix} M_{\varphi} \\ M_z \\ P_r \end{pmatrix} = \begin{pmatrix} \alpha_m H_{0\varphi} \\ 0 \\ \alpha_e \varepsilon E_{0r} \end{pmatrix}, \quad (8)$$

where we have defined

$$\begin{aligned} S_{\varphi\varphi} &= \frac{j\omega}{2} \sum (h_{i\varphi(n,m)}^2 - h_{e\varphi(n,m)}^2) \Big|_{\varphi=0}^{r=b}, \\ S_{\varphi z} &= \frac{j\omega}{2} \sum (h_{i\varphi(n,m)} h_{iz(n,m)} - h_{e\varphi(n,m)} h_{ez(n,m)}) \Big|_{\varphi=0}^{r=b}, \\ S_{\varphi r} &= \frac{j\omega}{2} \sum (h_{i\varphi(n,m)} e_{ir(n,m)} - h_{e\varphi(n,m)} e_{er(n,m)}) \Big|_{\varphi=0}^{r=b}, \\ S_{zz} &= \frac{j\omega}{2} \sum (h_{iz(n,m)}^2 - h_{ez(n,m)}^2) \Big|_{\varphi=0}^{r=b}, \\ S_{zr} &= \frac{j\omega}{2} \sum (h_{iz(n,m)} e_{ir(n,m)} - h_{ez(n,m)} e_{er(n,m)}) \Big|_{\varphi=0}^{r=b}, \\ S_{rr} &= \frac{j\omega}{2} \sum (e_{ir(n,m)}^2 - e_{er(n,m)}^2) \Big|_{\varphi=0}^{r=b}. \end{aligned} \quad (9)$$

### Coaxial structure

We now investigate the effect of the outer pipe of radius  $d$  on the coupling impedance. First consider the simple case of frequencies such that all TE and TM modes are below cutoff, so that there is propagation only in the coaxial waveguide. Under these conditions, the magnetic field can have only the component along  $\varphi$ , therefore, the linear system in (8) reduces to

$$\begin{pmatrix} 1 + \alpha_m \mu S_{\varphi\varphi} & \pm \alpha_m S_{\varphi r} \\ \pm \frac{\alpha_e}{c^2} S_{\varphi r} & 1 + \alpha_e \varepsilon S_{rr} \end{pmatrix} \begin{pmatrix} M_{\varphi} \\ P_r \end{pmatrix} = \begin{pmatrix} \alpha_m H_{0\varphi} \\ \alpha_e \varepsilon E_{0r} \end{pmatrix} \quad (10)$$

with

$$S_{\varphi\varphi} = \frac{j\omega}{2} h_{e0\varphi}^2 \Big|_{\varphi=0}^{r=b},$$

$$S_{\varphi r} = \frac{j\omega}{2} h_{e0\varphi} e_{e0r} \Big|_{\varphi=0}^{r=b},$$

$$S_{rr} = \frac{j\omega}{2} e_{e0r}^2 \Big|_{\varphi=0}^{r=b},$$

where we have indicated with the single subscript 0 the TEM modal functions. Solving (10) gives:

$$M_{\varphi} = \frac{\alpha_m H_{0\varphi}}{\Delta},$$

$$P_r = \frac{\alpha_e \varepsilon E_{0r}}{\Delta}, \quad (11)$$

$$\Delta = 1 - j \frac{kR}{6\pi} \frac{(R/b)^2}{\ln(d/b)},$$

The polarizability coefficients  $\alpha_e$ ,  $\alpha_m$  for a thin circular hole of radius  $R$  are equal to  $-2R^3/3$  and  $4R^3/3$ , respectively [1].

### III. LONGITUDINAL IMPEDANCE

The longitudinal impedance is defined by

$$Z_{\parallel}(\omega) = -\frac{2\pi}{q} \int_{-\infty}^{+\infty} E_z(r=0) e^{jk_0 z} dz, \quad (12)$$

$$k_0 = \frac{\omega}{\beta c}.$$

Only the  $TM_{0m}$ , having nonzero longitudinal electric field on the pipe axis, contribute to the impedance. After carrying out the integration for  $\beta=1$ , we get:

$$Z_{\parallel}(\omega) = -j \frac{\omega Z_0}{\pi q b} \left[ \frac{1}{c} M_{\varphi} + P_r \right] \sum_{m=1}^{\infty} \frac{1}{\xi_{0m} J_1(\xi_{0m})}. \quad (13)$$

The sum of the series in (13) is equal to 1/2, so that we recognize the impedance found by Kurennoy [1] but for the factor  $1/\Delta$  in the expressions for the dipole moments (11).

By substituting (11) and (A5) in (13), it is easy to show that at frequencies below the cutoff of  $g_i$  and  $g_e$  the condition

$$\omega \ll \frac{c \ln(d/b)}{R (R/b)^2}$$

is always fulfilled so that we can write:

$$Z_{\parallel}(\omega) \approx \frac{Z_0}{6\pi^2} kR (R/b)^2 \left[ -j + \frac{kR}{6\pi} \frac{(R/b)^2}{\ln(d/b)} \right]. \quad (14)$$

It is worth pointing out that the real part of the impedance behaves like  $\omega^2$ .

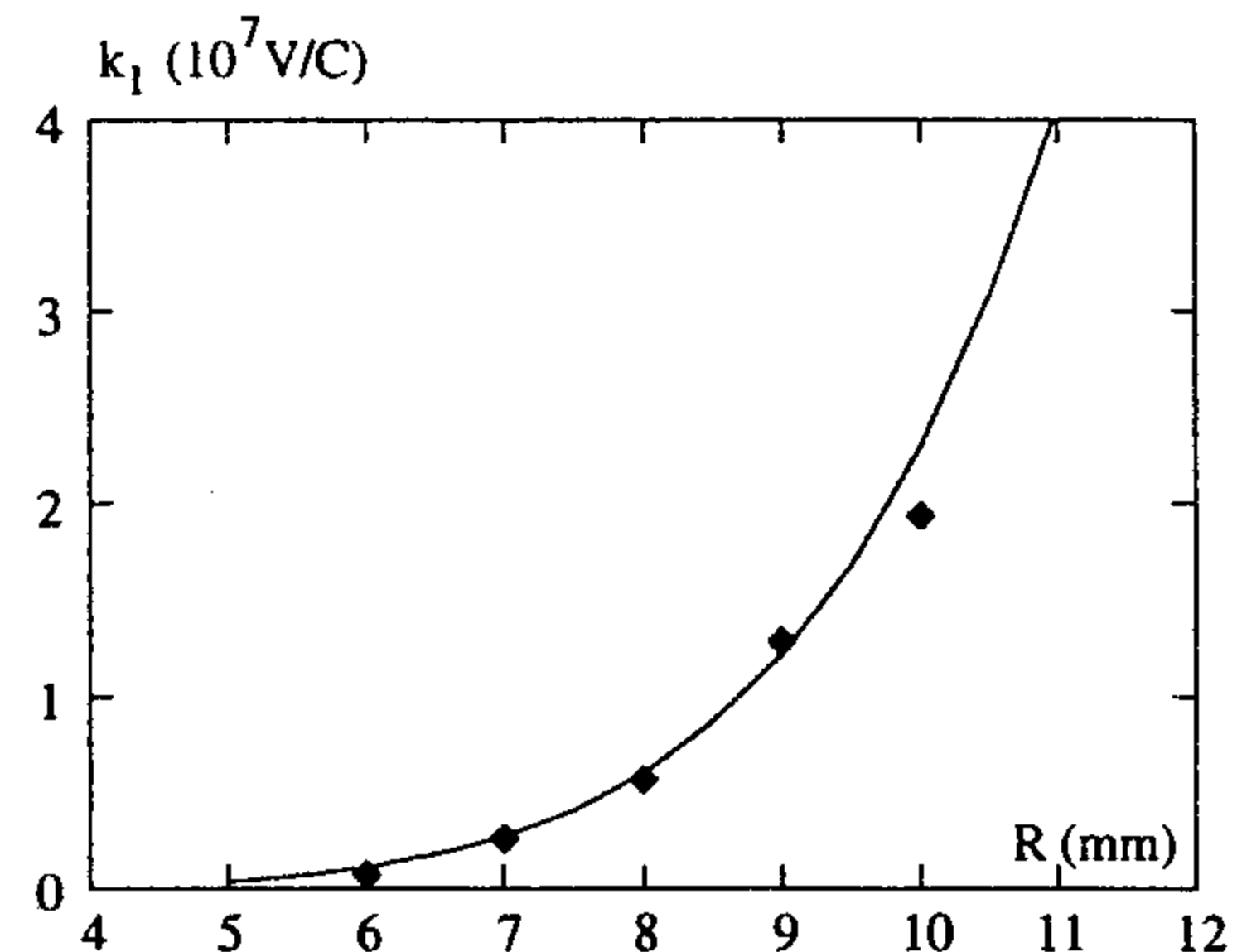


FIG. 2. Dependence of the loss factor on the hole radius.

### IV. NUMERICAL RESULTS

In order to check the validity of expression (14) we perform simulations with the numerical code MAFIA. To satisfy all the model approximations some limitations have to be fulfilled in the simulations:

(a) The radius of the hole has to be much smaller than the radius of the inner tube:  $R \ll 2\pi b$ .

(b) The inner tube wall thickness should be much smaller than the hole radius in order to prevent attenuation of the fields radiated outside the inner tube.

(c) The bunch spectrum must lie under the lowest cutoffs of the inner cylindrical tube and the coaxial formed by the inner and outer tubes.

(d) Both tubes must be long enough in order to simulate an infinitely long coaxial line. In our simulations the tube is much longer than the bunch length  $\sigma_z$  in the loss factor calculations.

Once we meet these conditions,  $(kR/6\pi)[(R/b)^2/\ln(d/b)]$  is  $\ll 1$  within all the bunch spectrum and the real part of the impedance can be written as:

$$\text{Re}\{Z(\omega)\} = Z_0 \left( \frac{\omega}{c} \right)^2 \frac{R^6}{36\pi^3 b^4 \ln(d/b)}. \quad (15)$$

Here we consider the case with  $d > b$  and not  $d \approx b$ . Applying the standard definition of the loss factor for the Gaussian bunch we have:

$$k_l(\sigma) = \frac{Z_0 \sqrt{\pi} R^6 c}{48\pi^4 b^4 \ln(d/b) \sigma_z^3}. \quad (16)$$

We compared the above analytical expression to the numerically calculated loss factor. Figure 2 shows the dependence of the loss factor of the Gaussian bunch with  $\sigma_z = 4$  cm on the hole radius. The inner tube radius is 2 cm and the outer one is 2.4 cm. The numerical results (black points) fit well the analytical dependence (solid line). Some small disagreement is observed at  $R = 10$  mm, when the hole radius is getting comparable to the inner pipe radius, i.e., when the model approximation no longer holds.

Figure 3 shows the dependence of the loss factor of the Gaussian bunch with  $\sigma_z = 5$  cm on the ratio of the pipe radii,  $d/b$ . The inner radius is constant and equal to 1 cm, the hole radius is 3 mm in the given set of simulations. As it can be seen, the analytical logarithmic dependence (16) is reasonably confirmed by the simulations.

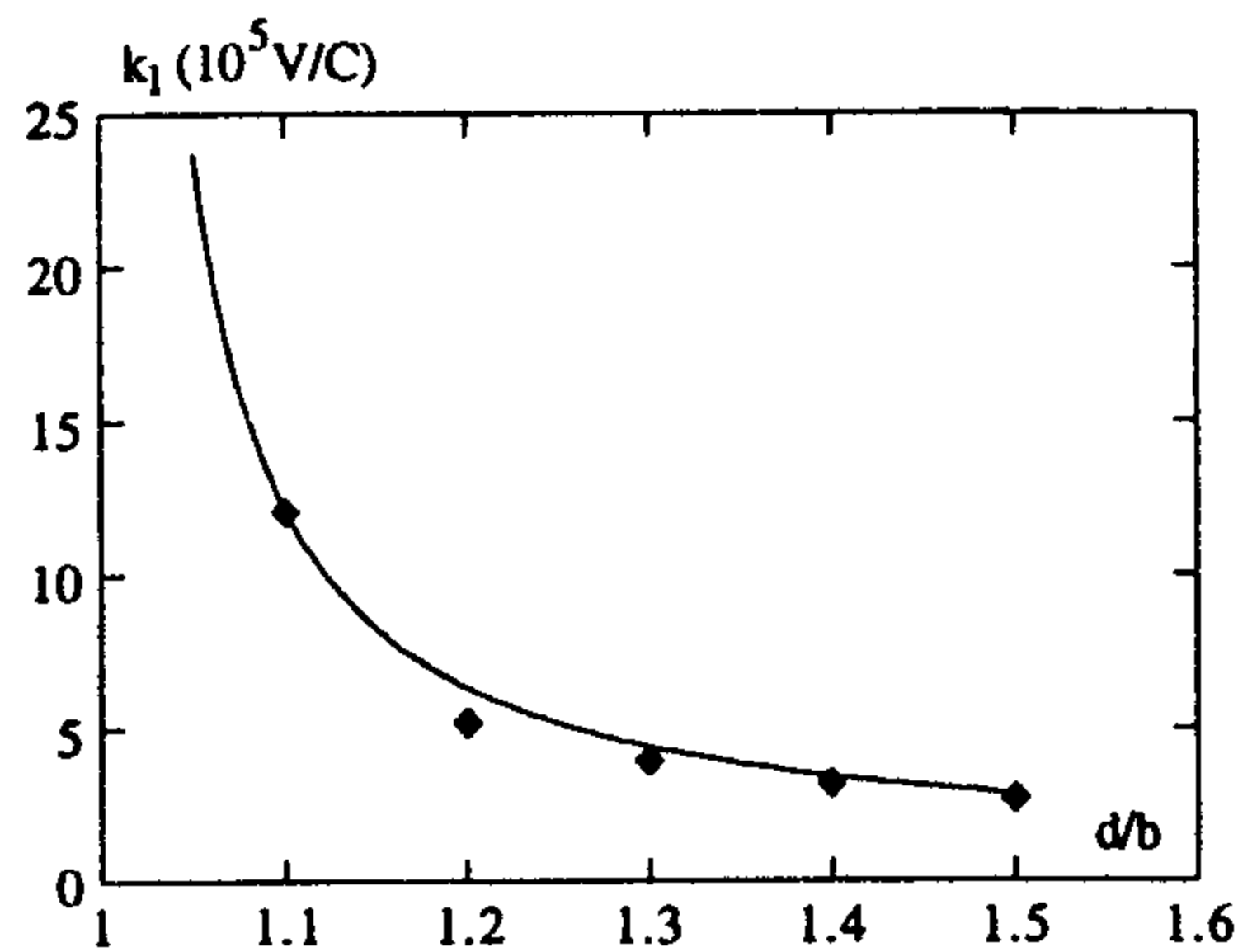


FIG. 3. Dependence of the loss factor on the ratio of the pipe radii.

### V. DIPOLE LONGITUDINAL AND TRANSVERSE IMPEDANCES

#### A. Longitudinal dipole impedance

The dipole field of a charge traveling with an offset  $(r_1, \varphi_1)$  at low frequency is

$$E_{0r}(r=b, \varphi=0) = \frac{qZ_0 r_1}{2\pi^2 b^2} \cos\varphi_1, \quad (17)$$

$$H_{0\varphi}(r=b, \varphi=0) = \frac{q}{2\pi^2 b^2} r_1 \cos\varphi_1.$$

Following a procedure similar to that of Kurennoy [1], we obtain:

$$Z_{\parallel}^{n=1}(r, \varphi) = j \frac{2\omega Z_0 R^3 r r_1 \cos\varphi \cos\varphi_1}{3\pi^2 c b^4 \Delta} \sum_m \frac{1}{J_0(\xi_{1,m})}, \quad (18)$$

where the  $\xi_{1,m}$  are the zeros of the first order Bessel's function  $J_1(x)$ . In Appendix C it is shown that the series in (18) can be analytically summed and it is equal to  $-1$ .

#### B. Transverse dipole impedance

The transverse impedance is defined by:

$$Z_{\perp}(\omega) = -\frac{j}{qr_1} \int_{-\infty}^{\infty} [(E_r - Z_0 H_{\varphi}) \hat{r} + (E_{\varphi} + Z_0 H_r) \hat{\varphi}] e^{jk_0 z} dz, \quad (19)$$

where the transverse field are those for the dipole fields ( $n=1$ ) given by (B1) and (B3) in the limit  $(r, \varphi) \rightarrow 0$ .

After some calculations, again we find the same expression as Kurennoy's except for the factor  $1/\Delta$ , namely:

$$Z_{\perp}(\omega) = -j \frac{2Z_0 R^3 \cos\varphi_1}{3\pi^2 b^4 \Delta} \times \left( 2 \sum_m \frac{\xi'_{1,m}}{(\xi'_{1,m}{}^2 - 1) J_1(\xi'_{1,m})} + \sum_m \frac{1}{J_0(\xi_{1,m})} \right) \hat{r}, \quad (20)$$

where the expression in brackets is equal to 1.

We remind that the above expression can be derived directly from the longitudinal impedance in (18) by applying the general relation between longitudinal and transverse impedances:

$$Z_{\perp} = \frac{c}{\omega r_1} \nabla_{\perp} Z_{\parallel}. \quad (21)$$

From (20) we see that the transverse impedance also exhibits a real part, which is linear with frequency.

### VI. IMPEDANCE FOR $\beta < 1$

In the case of a charge traveling with velocity  $v < c$ , the impedance is in general lower. Only the fields synchronous with the charge (i.e., with the same phase velocity) can contribute to the impedance. This effect is accounted for by evaluating the integrals (12) and (19) assuming  $k_0 = \omega/\beta c$ .

The final expressions are

$$Z_{\parallel}(\omega) = -j \frac{2\omega Z_0}{qb} \beta \left[ \frac{\beta}{c} M_{\varphi} - P_r \right] \times \sum_m \frac{1}{J_1(\xi_{0,m}) \xi_{0,m}} \left[ \left( \frac{kb}{\gamma \xi_{0,m}} \right)^2 + \beta^2 \right]^{-1} \quad (22)$$

and

$$Z_{\perp}(\omega) = -j \frac{2Z_0 \beta c}{qb^2 r_1} \left[ \frac{\beta}{c} M_{\varphi} - P_r \right] \sum_{m=1}^{\infty} \frac{1}{J_0(\xi_{1,m})} \times \left[ \left( \frac{kb}{\gamma \xi_{1,m}} \right)^2 + \beta^2 \right]^{-1} \hat{r}. \quad (23)$$

### VII. CONCLUSIONS

We have calculated the coupling impedance of a pumping hole on a coaxial beam pipe at low frequency. It has been shown that, applying a modified Bethe's diffraction theory which accounts for the power loss, the longitudinal and transverse impedances have a resistive term. Numerical calculations confirm the analytical results.

### APPENDIX A

The fields produced by a point charge traveling inside a perfectly conducting cylindrical pipe with velocity  $\mathbf{v} = \beta c \mathbf{z}$  are found from the scalar potential  $V(r, \varphi, z - vt)$  solution of the Maxwell equations with homogeneous boundary conditions at the pipe wall  $r = b$  [12].

In cylindrical coordinates we can express this potential as a sum of multipole terms:

$$V(r, \varphi, z - vt) = \frac{1}{2\pi} \sum_{n=0}^{\infty} \cos(n\varphi) \times \int_{-\infty}^{\infty} \tilde{V}_n(r, r_1, k_0) e^{-jk_0(z-vt)} dk_0, \quad (\text{A1})$$

where we made use of the Fourier transform from the  $z$  space

to the wave-number domain  $k$ . Each Fourier component is obtained by solving the differential equation

$$\nabla_{\perp} V + \frac{1}{\gamma^2} \frac{\partial V}{\partial z} = -\frac{\rho}{\epsilon}, \quad (\text{A2})$$

where  $\gamma = (1 - \beta^2)^{-1/2}$ . Imposing the boundary conditions at the pipe walls, we get:

$$\tilde{V}_n(r, r_1, k_0) = \frac{q\epsilon_n}{2\pi\epsilon} \begin{cases} K_n(\chi r) I_n(\chi r_1) - \frac{I_n(\chi r_1)}{I_n(\chi b)} K_n(\chi b) I_n(\chi r), & r \geq r_1 \\ K_n(\chi r_1) I_n(\chi r) - \frac{I_n(\chi r_1)}{I_n(\chi b)} K_n(\chi b) I_n(\chi r), & r_1 \geq r, \end{cases} \quad (\text{A3})$$

where  $\chi = k_0/\beta\gamma$ ,  $I_n$  and  $K_n$  are the modified Bessel's functions, and  $\epsilon_n$  is Neumann's symbol (1 if  $n=0$ , 2 if  $n>0$ ).

The electric field can be obtained from

$$\mathbf{E} = -\frac{1}{\gamma^2} \frac{\partial V}{\partial z} \hat{\mathbf{z}} - \nabla_{\perp} V. \quad (\text{A4})$$

From (A3) and (A4) it is easy to see that for a relativistic charge the low-frequency monopolar fields on the aperture are

$$\mathbf{E}_{or}^{n=0}(r=b, \varphi=0) = Z_0 \frac{q}{2\pi b} \hat{\mathbf{r}}, \quad (\text{A5})$$

$$\mathbf{H}_{o\varphi}^{n=0}(r=b, \varphi=0) = \frac{q}{2\pi b} \hat{\boldsymbol{\varphi}},$$

while the corresponding dipole fields are given by

$$\mathbf{E}_{or}^{n=1}(r=b, \varphi=0) = Z_0 \frac{q}{2\pi^2} \frac{r_1}{b^2} (\cos\varphi_1) \hat{\mathbf{r}}, \quad (\text{A6})$$

$$\mathbf{H}_{o\varphi}^{n=1}(r=b, \varphi=0) = \frac{q}{2\pi^2} \frac{r_1}{b^2} (\cos\varphi_1) \hat{\boldsymbol{\varphi}}.$$

For  $\beta < 1$  there is also a component of the electric field along  $z$ . However, we do not give its expression since it never couples with the aperture.

## APPENDIX B

### Circular waveguide ( $g_i$ )

#### TE modes

$$e_r = -C_{n,m} \frac{n}{r} J_n(k_{t(n,m)} r) \cos(n\varphi), \quad (\text{B1})$$

$$e_{\varphi} = C_{n,m} k_{t(n,m)} J'_n(k_{t(n,m)} r) \sin(n\varphi),$$

$$e_z = 0,$$

$$h_r = -C_{n,m} \frac{k_{t(n,m)} k_{z(n,m)}}{\omega\mu} J'_n(k_{t(n,m)} r) \sin(n\varphi),$$

$$h_{\varphi} = -C_{n,m} \frac{k_{z(n,m)} n}{\omega\mu r} J_n(k_{t(n,m)} r) \cos(n\varphi),$$

$$h_z = C_{n,m} \frac{k_{t(n,m)}^2}{j\omega\mu} J_n(k_{t(n,m)} r) \sin(n\varphi).$$

The normalization constant  $C_{n,m}$  is given by:

$$\frac{1}{C_{n,m}^2} = \frac{\pi k_{z(n,m)}}{\omega\mu} \left[ (1 + \delta_{n0}) n^2 \int_0^b J_n^2(k_{t(n,m)} r) \frac{dr}{r} + (1 - \delta_{n0}) k_{t(n,m)}^2 \int_0^b J_n'^2(k_{t(n,m)} r) r dr \right]. \quad (\text{B2})$$

For the TE modes the  $k_t$ 's are the zeros of  $J'_n(\xi'_{n,m})$  divided by  $b$ .

#### TM modes

$$e_r = -C_{n,m} \frac{k_{t(n,m)}}{\omega\epsilon} J'_n(k_{t(n,m)} r) \cos(n\varphi),$$

$$e_{\varphi} = C_{n,m} \frac{1}{\omega\epsilon} \frac{n}{r} J_n(k_{t(n,m)} r) \sin(n\varphi),$$

$$e_z = C_{n,m} \frac{1}{j\omega\epsilon} \frac{k_{t(n,m)}^2}{k_{z(n,m)}} J_n(k_{t(n,m)} r) \cos(n\varphi), \quad (\text{B3})$$

$$h_r = -C_{n,m} \frac{1}{k_{z(n,m)}} \frac{n}{r} J_n(k_{t(n,m)} r) \sin(n\varphi),$$

$$h_{\varphi} = -C_{n,m} \frac{k_{t(n,m)}}{k_{z(n,m)}} J'_n(k_{t(n,m)} r) \cos(n\varphi),$$

$$h_z = 0.$$

For TM modes,  $C_{n,m}$  is

$$\frac{1}{C_{n,m}^2} = \frac{\pi}{\omega \epsilon k_{z(n,m)}} \left[ (1 - \delta_{n0}) n^2 \int_0^b J_n^2(k_{t(n,m)} r) \frac{dr}{r} + (1 + \delta_{n0}) k_{t(n,m)}^2 \int_0^b J_n'^2(k_{t(n,m)} r) r dr \right] \quad (\text{B4})$$

and the  $k_t$ 's are  $1/b$  times the zeros of  $J_n(\xi_{n,m})$ .

### Coaxial Waveguide ( $g_e$ )

#### TEM mode

$$e_{e0r} = \sqrt{Z_0/2\pi} \frac{1}{\sqrt{\ln(d/b)}} \frac{1}{r},$$

$$h_{e0\phi} = \frac{1}{Z_0} e_{e0r}. \quad (\text{B5})$$

TE and TM modes for  $g_e$  can be obtained from the correspondent  $g_i$  modes simply substituting  $[J_n]$  to  $J_n$  and  $[J_n']$  to  $J_n'$ , where we have defined:

$$[J_n] = J_n(k_{t(n,m)} r) + \begin{cases} -\frac{J_n'(k_{t(n,m)} b)}{Y_n'(k_{t(n,m)} b)} Y_n(k_{t(n,m)} r) & (\text{TE}) \\ -\frac{J_n(k_{t(n,m)} b)}{Y_n(k_{t(n,m)} b)} Y_n(k_{t(n,m)} r) & (\text{TM}), \end{cases} \quad (\text{B6})$$

$$[J_n'] = J_n'(k_{t(n,m)} r) + \begin{cases} -\frac{J_n'(k_{t(n,m)} b)}{Y_n'(k_{t(n,m)} b)} Y_n'(k_{t(n,m)} r) & (\text{TE}) \\ -\frac{J_n(k_{t(n,m)} b)}{Y_n(k_{t(n,m)} b)} Y_n'(k_{t(n,m)} r) & (\text{TM}). \end{cases}$$

The  $k_t$ 's in (B6) are  $1/b$  times the zeros of  $[J_n']$  (TE modes) and of  $[J_n]$  (TM modes), calculated for  $r=b$ .

### APPENDIX C

To calculate the sum in (18), we make use of the relation [13]:

$$\frac{1}{J_0(\xi_{1,m})} = 2 \sum_{k=1}^{\infty} \frac{\xi_{0,k}}{(\xi_{0,k}^2 - \xi_{1,m}^2) J_1(\xi_{0,k})}. \quad (\text{C1})$$

From (18) and (C1), exchanging the order of summation, one gets:

$$\sum_{m=1}^{\infty} \frac{1}{J_0(\xi_{1,m})} = 2 \sum_{k=1}^{\infty} \frac{\xi_{0,k}}{J_1(\xi_{0,k})} \sum_{m=1}^{\infty} \frac{1}{\xi_{0,k}^2 - \xi_{1,m}^2}. \quad (\text{C2})$$

The second sum in the right-hand side of (C2) is equal to  $-(1/2)J_2(\xi_{0,m})/J_1(\xi_{0,m})$  so that the above equation reduces to

$$\sum_{m=1}^{\infty} \frac{1}{J_0(\xi_{1,m})} = -2 \sum_{k=1}^{\infty} \frac{J_2(\xi_{0,k})}{J_1^2(\xi_{0,k})}, \quad (\text{C3})$$

which, given the properties of Bessel's functions, is finally equal to

$$\sum_{m=1}^{\infty} \frac{1}{J_0(\xi_{1,m})} = -2 \sum_{k=1}^{\infty} \frac{1}{\xi_{0,k} J_1(\xi_{0,k})} = -1. \quad (\text{C4})$$

- [1] S. S. Kurennoy, Part. Acc. **39**, 1 (1992).  
 [2] R. L. Gluckstern, CERN Report No. SL/92-05 (AP) (1992).  
 [3] R. L. Gluckstern, Phys. Rev. A **46**, 1110 (1992).  
 [4] S. S. Kurennoy, SSCL Report No. 636 (1993).  
 [5] S. S. Kurennoy, in *Proceedings of the 4th EPAC* (World Scientific, Singapore, 1994), Vol. 2, p. 1286.  
 [6] S. S. Kurennoy, Part. Acc. **50**, 167 (1995).  
 [7] F. Ruggiero (private communication).  
 [8] R. E. Collin, *Field Theory of Guided Waves*, 2nd ed. (IEEE, New York, 1991).

- [9] G. V. Stupakov, Phys. Rev. E **51**, 3515 (1995).  
 [10] R. L. Gluckstern, S. S. Kurennoy, and G. V. Stupakov, Phys. Rev. E **52**, 4354 (1995).  
 [11] S. S. Kurennoy (unpublished).  
 [12] L. Palumbo and V. G. Vaccaro, CAS Advanced Accelerator School, CERN 87-D3 (1987).  
 [13] *Higher Transcendental Functions*, edited by A. Erdelyi (McGraw-Hill, New York, 1953), Vol. 2.